Bull. Chem. Soc. Jpn., **68**, 1226—1231(1995)

Catalytic Decomposition of Dinitrogen Oxide over Perovskite-Related Mixed Oxides

Jie Wang, Hiroyuki Yasuda,# Kei Inumaru, and Makoto Misono*

Department of Applied Chemistry, Faculty of Engineering, The University of Tokyo, Bunkyo-ku, Tokyo 113

(Received October 3, 1994)

The catalytic decomposition of dinitrogen oxide (N_2O) was carried out over $La_{2-x}Sr_xCuO_4$ (x=0—1), $LaMO_3$ (M=Cr, Mn, Fe, Co, and Ni) and La_2MO_4 (M=Co, Ni, and Cu) mixed oxides with perovskite and perovskite-related structure. The reaction rate at the steady state was first-order in the partial pressure of N_2O, with reversible inhibition of oxygen. The initial rate was enhanced by pretreatment in helium at 1073 K, but decreased gradually due to irreversible inhibition of oxygen formed by the reaction, while the rate increased with time when the catalyst was pretreated in oxygen. A good correlation between the catalytic activity and the average oxidation number of copper (AON) was observed for $La_{2-x}Sr_xCuO_4$ and was explained by a Cu^{2+}/Cu^{3+} redox mechanism. The catalytic activity for a series of $LaMO_3$ and La_2MO_4 showed a one peak pattern with Co at the peak. These trends in catalytic activity are similar in general to those for NO decomposition.

The decomposition of N_2O has been studied mostly as a model reaction for the elucidation of the mechanism of catalysis.[1—8] Catalysts investigated so forth range from metals,[1,2] oxides[3—6] to zeolites.[7,8] Recently, N_2O has been realized to be an environmental pollutant, because accumulated evidence shows that it contributes to stratospheric ozone destruction and greenhouse effects.[9] With this concern, there is urgent need to abate N_2O emission into the atmosphere.[10]

Perovskite-related mixed oxides are known for their structural stability and variable composition, as the nonstoichiometry of oxygen or the valency of metal ions can be controlled in a regular way. Therefore, they are suitable model compounds for the study of the relationships between the solid state chemistry of catalyst and the catalytic function.[11—13]

In our previous paper,[14] the catalytic activity for the decomposition of NO over valency-controlled La_2CuO_4-based mixed oxides was correlated well with the valency of copper; the catalysts of which the average oxidation number (AON) of copper was greater than 2 exhibited very high activity. It was also shown that there were reversibly and irreversibly adsorbed oxygen species and both of them significantly suppressed the NO decomposition.

In the present work we attempted to elucidate the relationships in the case of the catalytic decomposition of N_2O. In addition, the effect of transition metal ions at B site was examined for several perovskites and compared with the results in the literature for NO decomposition.

Experimental

Catalysts. The $LaMO_3$ (M: transition elements) catalysts except for $LaFeO_3$ were prepared from metal acetates in the same manner as has been described previously.[14] The precipitates, which had been obtained from mixed acetate solutions by evaporation to dryness in a rotary evaporator, were decomposed in air at 573 K for 3 h. After sufficient grinding in a mortar, they were calcined again in air at 1173 K for 10 h. La_2CoO_4 and La_2NiO_4 were also prepared from coprecipitation of metal acetates in a similar way, but precursors were calcined in nitrogen in stead of air at 1173 K for 10 h, according to the literature.[15] $LaFeO_3$ was synthesized from a mixture of nitrates of each component following the literature.[16] The precipitates were obtained from the mixed nitrate solution by adding butylamine. After they were filtrated and decomposed at 573 K in air, the precursor was calcined in air at 1173 K. The structure was checked by powder X-ray diffractometer (Rigaku Denki, Rotaflex, RU-2000) using Cu $K\alpha$ radiation. The surface areas of the samples were measured by means of the BET method (N_2 adsorption).

Apparatus. The decomposition of N_2O was carried out in a fixed-bed flow reactor at atmospheric pressure. A quartz glass tube (8 mm in inside diameter) was used as a reactor. The temperature was monitored by a chromel–alumel thermocouple. The gas compositions at the both inlet and outlet of the reactor were analyzed by gas chromatography (a molecular sieve 5A column, 1.5 m, for N_2 and O_2; a Porapak® Q column, 3 m, for N_2O; both at 328 K). Prior to the reaction, the catalysts (0.6 g in most cases) were usually pretreated in He or O_2 stream for 1 h at 1073 K, and the temperature was lowered to the reaction temperature in the same atmosphere. The reaction gas, which was 1000 ppm

#Present address: Chemical Technology Division, Institute of Research and Innovation, Takada 1201, Kashiwa, Chiba 227.

N_2O in He, was supplied onto the catalyst at a flow rate of 120 cm^3 min^{-1} (contact time: usually 0.3 g s cm^{-3}).

Results

Bulk Structure and Physicochemical Properties. The crystal structure and specific surface area of the catalysts are summarized in Table 1. The structure was confirmed for all the catalysts with reference to ASTM cards. Since both XRD patterns and surface areas for $La_{2-x}Sr_xCuO_4$ were very close to those in the previous study,[14] it may be reasonable to quote the average oxidation numbers (AON) of copper, which was determined by iodometry previously.[14] AON increased with the Sr substitution upto $x=0.5$. Oxygen vacancy, δ, was calculated according to the principle of electric neutrality.

The Kinetics and the Effects of Pretreatment. The initial rate of the N_2O decomposition changed depending on pretreatment, but it reached a nearly stationary state after a certain period (see later section). The stoichiometry of $N_2O \rightarrow N_2 + \frac{1}{2}O_2$ held at the later stage. The dependency of the stationary rate on the contact time (W/F; W=catalyst weight, F=flow rate) is shown in Fig. 1 for $La_{1.8}Sr_{0.2}CuO_4$ at 723 K. The % conversion tended to be saturated when W/F was high. This is mainly due to the inhibition of oxygen, as it will be quantitatively discussed in the later section. The plots for 0.6 and 1.0 g of catalysts agreed, while the curve for 0.3 g was lower. This indicates that under the standard reaction conditions ($W=0.6$ g, $F=120$ cm^3 min^{-1}; $W/F=0.3$ g s cm^{-3}), the rate of overall reaction was not controlled by the mass transport through boundary layer.

Table 1. Structure, Specific Surface Area of Catalysts, Average Oxidation Number (AON) of Copper, and δ of $La_{2-x}Sr_xCuO_{4-\delta}$

Catalyst	Structure[a]	Surface area/m^2 g^{-1}	AON of copper[b]	δ[b]
$La_2Cu_{0.9}Zr_{0.1}O_4$	K(O)	3.6	1.84	−0.04
La_2CuO_4	K(O)	1.2	2.00	0.00
$La_{1.9}Sr_{0.1}CuO_4$	K(T)	1.3	2.10	0.00
$La_{1.8}Sr_{0.2}CuO_4$	K(T)	1.1	2.20	0.00
$La_{1.6}Sr_{0.4}CuO_4$	K(T)	1.7	2.22	0.09
$La_{1.5}Sr_{0.5}CuO_4$	K(T)	1.3	2.30	0.10
$La_{1.2}Sr_{0.8}CuO_4$	K(T)	1.4	2.16	0.32
$LaSrCuO_4$	K(T)[d]	1.2	2.21	0.40
$LaCrO_3$	P(O)	3.5	—	—
$LaMnO_3$	P(R)	2.5	—	—
$LaFeO_3$	P(O)	4.9	—	—
$LaCoO_3$	P(O)	3.1	—	—
$LaNiO_3$	P(R)	2.5	—	—
La_2CoO_4[c]	K(O)	3.4	—	—
La_2NiO_4	K(T)	4.0	—	—

a) K: K_2NiF_4-type structure, P: Perovskite, O: Orthorhombic, T: Tetragonal, R: Rhombohedral. b) From Ref. 14. c) Calcined in nitrogen. d) See Ref. 14.

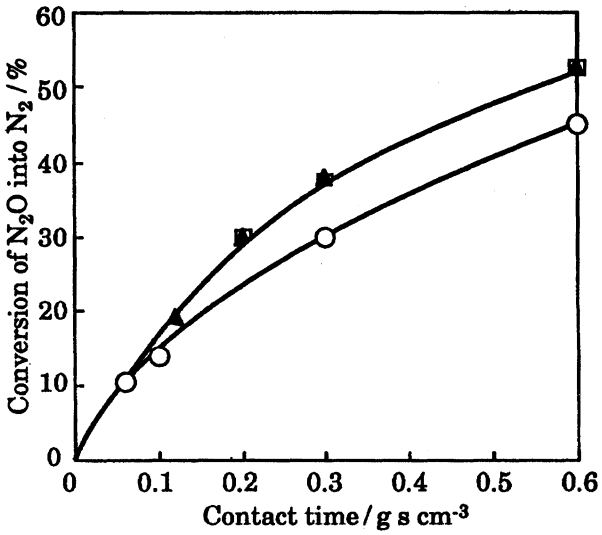

Fig. 1. Dependency of the conversion of N_2O decomposition on the contact time over $La_{1.8}Sr_{0.2}CuO_4$ at 773 K. ○, ▲, and □ correspond to catalyst weight 0.3, 0.6, and 1.0 g, respectively.

Figure 2 shows the dependence of the conversion on the partial pressure of N_2O (500—10,000 ppm) for $La_{1.8}Sr_{0.2}CuO_4$ at 723 K. Open circles and solid line are experimental results, while solid symbols are results simulated by the rate equations which will be discussed in later section. The conversion decreased slightly with the increase of the partial pressure of N_2O. The apparent reaction order with respect to N_2O, which was obtained from a plot of log of rate vs. log of pressure, was about 0.8. The influence of oxygen mixed into the feed gas on the stationary conversion was also examined.

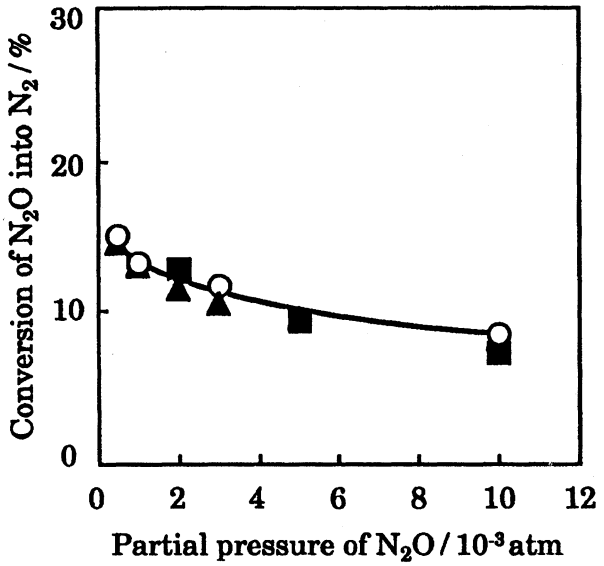

Fig. 2. Dependency of the conversion of N_2O decomposition on the pressure of N_2O over $La_{1.8}Sr_{0.2}CuO_4$ at 773 K, $W/F=0.06$ g s cm^{-3}. ○: observed. ■ and ▲ correspond to the calculated values from Eqs. 6 and 7, respectively.

The results are shown in Fig. 3 (open circle). Solid symbols are from simulation (see below). The decomposition of N_2O was suppressed by the coexistence of oxygen, the apparent reaction order varying from about -0.7 to -0.2 in the partial pressure of oxygen from 250 to 10000 ppm. The effect was reversible upon the elimination of oxygen from the feed gas.

The effects of pretreatment by oxygen or helium at 1073 K for $La_{1.8}Sr_{0.2}CuO_4$ are shown in Fig. 4. The reactant (N_2O 1000 ppm in He) was introduced into the reactor at 873 K (a) or 723 K (b) after the catalyst had been pretreated for 1 h in different atmospheres.

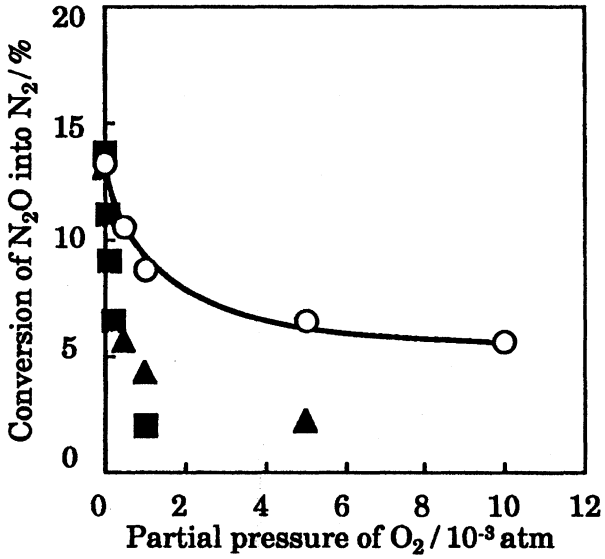

Fig. 3. Dependency of the conversion of N_2O decomposition on oxygen pressure at 773 K, $W/F=0.06$ g s cm^{-3}. ○: observed. ■ and ▲ correspond to the calculated values from Eqs. 6 and 7, respectively.

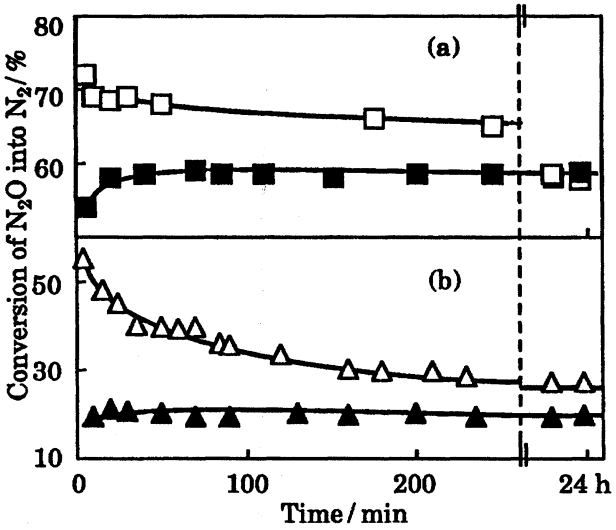

Fig. 4. Effects of pretreatments in He (□, △) and O_2 (■, ▲) at 1073 K on N_2O decomposition over $La_{1.8}Sr_{0.2}CuO_4$. (a) $W/F=0.025$ g s cm^{-3}, at 873 K; (b) $W/F=0.3$ g s cm^{-3}, at 723 K.

After the treatment in helium, the conversion of N_2O into N_2 was initially high, but it decreased rapidly and reached slowly a stationary value. Oxygen was not detected at the outlet in the first 10 min and then it rose to the value satisfying the stoichiometry of the reaction, $N_2O \rightarrow N_2 + \frac{1}{2}O_2$, in about 1 h. The conversion continued to decrease slowly thereafter, but the imbalance of oxygen was not detected beyond the experimental error (100±2%).

In contrast, the activity of the catalyst pretreated in an oxygen stream became constant rapidly. The rate at steady state at 723 K was considerably lower than that treated in helium even after 24 h. On the other hand, at 873 K the activities for the two pretreatments became equal after 24 h of reaction. By the treatment of the used catalyst in helium at 1073 K, the catalytic activity was recovered to the original level.

The Effects of Sr Substitution at A-Site on the Catalytic Activity. The effect of the valency control by means of Sr substitution was examined for $La_{2-x}Sr_xCuO_4$. Results are shown in Fig. 5, together with AON of copper. Here the catalytic activity is expressed by the % conversion divided by the surface area, where the % conversion ranged from 10 to 40%. The activity was initially enhanced by substituting La by Sr and then decreased, a maximum being observed at $x=0.5$. Parallelism between the activity and AON may be noted. The correlation is further confirmed in Fig. 6, where $La_2Cu_{0.9}Zr_{0.1}O_4$ is included. The activity monotonically increased with the increase of AON. This trend is similar to that found previously for the decomposition of NO.[14]

The Effects of 3d Transition Elements at B-Site in $LaMO_3$ and La_2MO_4 on the Catalytic Activity. Catalytic activities of $LaMO_3$ and La_2MO_4 mixed oxides for N_2O decomposition, which are plotted against the sequence of transition elements in the fourth

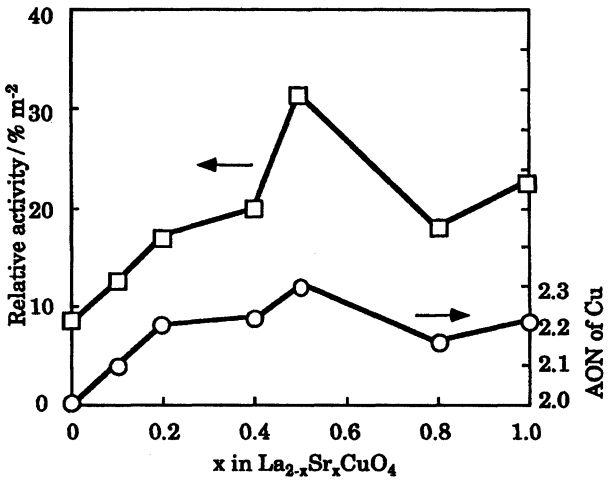

Fig. 5. Relative activities for N_2O decomposition (723 K, $W/F=0.3$ g s cm^{-3}) and the average oxidation number (AON) of copper for $La_{2-x}Sr_xCuO_4$.

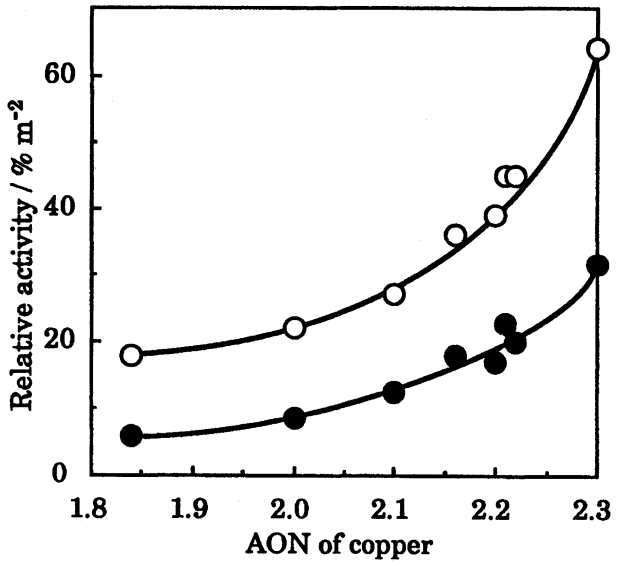

Fig. 6. Correlation between the activity for N_2O decomposition and the average oxidation number (AON) of copper for $La_{2-x}Sr_xCuO_4$ at 723 K (●) and 773 K (○), W/F=0.3 g s cm^{-3}.

period, are shown in Fig. 7. A one-peak pattern was obtained with Co at peak. $LaCoO_3$ was about 40 and 20 times more active than $LaMnO_3$ and $LaFeO_3$. The apparent activation energy was calculated from the slope of the plot of log (% conversion) against $1/T$, where the conversion was controlled below 30%. These results are listed in the column B of Table 2. The activation energy was in the order $LaCoO_3$ < $LaNiO_3$ < $LaFeO_3$ < $LaMnO_3$ < $LaCrO_3$. Activation energies in column A of Table 2 were calculated in a more precise way by considering the rate equation, as well (see below).

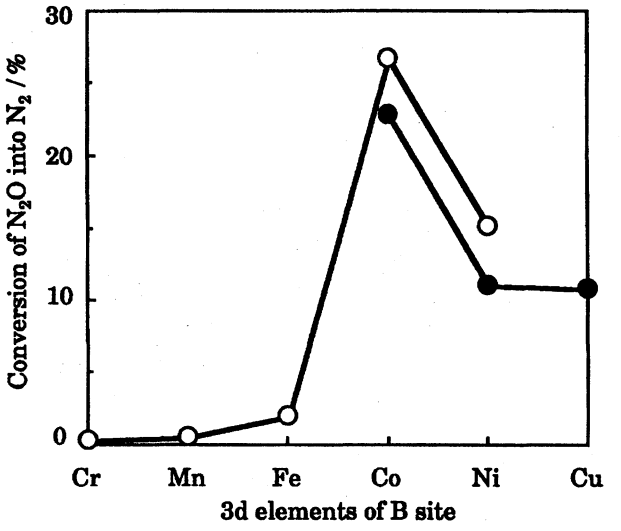

Fig. 7. Activity profiles of N_2O decomposition over $LaMO_3$ (○) and La_2MO_4 (●) at 723 K, W/F=0.3 gm s cm^{-3}.

Table 2. Apparent Activation Energy of N_2O Decomposition

Catalyst	Activation energy/kJ mol^{-1}	
	A	B
$LaCrO_3$	119	117
$LaMnO_3$	120	121
$LaFeO_3$	127	126
$LaCoO_3$	37.3	39.0
$LaNiO_3$	77.0	76.8
$La_{1.9}Sr_{0.1}CuO_4$	—	169
$La_{1.6}Sr_{0.4}CuO_4$	—	87.5
$La_{1.5}Sr_{0.5}CuO_4$	—	97.7

A) Calculated from the rate constant, k_2 (see text).
B) Calculated from log (% conversion) vs. $1/T$ at W/F=0.3 g s cm^{-3}.

Discussion

Surface Oxidation State and the Catalytic Activity. Catalytic oxidation reactions on metal oxide are generally sensitive to the oxidation state of catalyst surface as well as adsorbed oxygen species. The dissociation of N_2O proceeds readily at oxygen vacancies of oxides, or at coordinatively unsaturated metal ions on the surface.[3,17] Therefore, the results shown in Fig. 4 can reasonably be explained as follows. On pretreatment with helium at 1073 K, the surface and lattice oxygen atoms of the catalyst are partly removed. N_2O molecule dissociates easily on this partially reduced surface to form N_2 and surface oxygen species. The rate of N_2O decomposition decreases rapidly, as the result of irreversible reoxidation of the surface by the oxygen formed by the reaction. In the case of the oxygen-pretreated catalyst, most of the active sites are already occupied by oxygen species or the surface is in a highly oxidized state. N_2O decomposition takes place on the remaining active site available on this oxidized surface, so that the activity is much lower than that of the He-treated catalyst.

These effects of pretreatment are similar to the case of NO decomposition.[14] A difference is that the change of the activity with time is much slower in the case of N_2O decomposition as compared with the NO decomposition. At 723 K, the rate of He-treated catalyst surface continued to decrease for a long period (Fig. 4b), and gave a different activity from that of O_2-treated catalyst. This is possibly because of the differences in the reaction temperature and in the partial pressure of O_2. At 873 K, as shown in Fig. 4a, the catalytic activities became equal and constant after 24 h. When the temperature is higher, the diffusion of oxygen in perovskite or the surface lattice relaxation would be easier.

After the catalytic decomposition reached a steady-state, the retarding effect of the coexisting of O_2 was reversible as shown in Fig. 3. Thus, there are apparently two kinds of oxygen species, as in the case of NO decomposition;[14] one is irreversible, and the other re-

versible, although the borderline between the two may not be distinct.

The Rate Equation of N_2O Decomposition. The decomposition of N_2O on oxides is usually described by the mechanism shown by Eqs. 1, 2, and 3.[3,19]

$$N_2O \rightleftharpoons N_2O(ads), \quad (1)$$

$$N_2O(ads) \rightarrow N_2 + O(ads), \quad (2)$$

$$2O(ads) \rightleftharpoons O_2. \quad (3)$$

The apparent reaction order with respect to N_2O obtained from a log–log plot was about 0.8 (Fig. 2), so that it may be reasonable to assume that the reaction order of N_2O is first-order, if one considers that the reaction is inhibited by oxygen formed by the reaction and this reduces the apparent dependency of the rate on N_2O pressure. Then the following rate expressions are derived based on simple Langmiur–Hinshelwood kinetics.

$$-\frac{dP_{N_2O}}{dt} = k_1 \frac{P_{N_2O}}{1 + bP_{O_2}^{\frac{1}{2}}}, \quad (4)$$

$$-\frac{dP_{N_2O}}{dt} = k_2 \frac{P_{N_2O}}{1 + b'P_{O_2}}. \quad (5)$$

In Eq. 4, N_2O decomposition is inhibited by dissociated oxygen species which is in equilibrium with gaseous oxygen. In Eq. 5, adsorbed diatomic oxygen species[20] inhibits the reaction. These two rate expressions are integrated to Eqs. 6 and 7, respectively.

$$\frac{W}{F} = \frac{1}{k_1 RT}\left\{[-\ln(1-x)] + b\sqrt{\frac{P_{N_2O}^0}{2}}\int_0^x \frac{\sqrt{x}}{1-x}dx\right\}, \quad (6)$$

$$\frac{W}{F} = \frac{1}{k_2 RT}\left\{[-\ln(1-x)] + \frac{b'P_{N_2O}^0}{2}[-\ln(1-x) - x]\right\}. \quad (7)$$

Here x represents the conversion of N_2O. These two equations were checked by the data in Fig. 1. A good linear correlations were obtained for both Eqs. 6 and 7 respectively. Hence, it is difficult to tell which one is the most fitted rate expression. Both Eq. 6 (b=1.5×10^3 atm$^{-\frac{1}{2}}$, k_1=0.37) and Eq. 7 (b'=9×10^3 atm^{-1}, k_2=2.9) also reproduced the dependency of the reaction rate on the pressure of N_2O observed experimentally (Fig. 2).

However, neither Eq. 6 nor Eq. 7 was able to simulate the dependency on the oxygen pressure as seen in Fig. 3. Calculated values are considerably lower than the experimental values except for P_{O_2}=0. This clearly demonstrates that the surface is highly heterogeneous for O_2 or O adsorption, and that the assumption of constant b or b' is not correct. This is in agreement with the observation that the apparent reaction order in P_{O_2} sharply decreased with increase in P_{O_2} from −0.7 to −0.2, as described above for the log–log plot of the data in Fig. 3. The coefficient b' calculated with Eq. 7 from the data at the pressure of oxygen of about 250 ppm was 6×10^3 and it was 1 for about 10000 ppm.

The dependencies of the conversion on contact time were also investigated on $LaMO_3$ at various temperatures. After the rate constants were calculated by using Eq. 6, the activation energies were obtained from the slopes of Arrhenius plots as listed in the column A of Table 2. They are close to the data calculated simply from the conversions given in the column B.

Controlling Factors of Catalytic Activity. (1) Effects of AON of Cu over $La_{2-x}Sr_xCuO_4$. A good correlation is noted between the catalytic activities for N_2O decomposition and the average oxidation number of copper (AON) for $La_{2-x}Sr_xCuO_4$, as shown in Fig. 6. This trend generally agrees with that observed previously for NO decomposition over the same catalysts.[14] The agreement implies that the AON of copper is also the main factor controlling the activity of N_2O decomposition. Oxygen vacancy which increases monotonically with the Sr substitution has apparently poor correlation with the catalytic activity as in the case of NO decomposition. Although the oxygen vacancy generated by pretreatment has strong effect on N_2O decomposition (Fig. 4), it is not the primarily dominating factor of the steady-state activity for a series of $La_{2-x}Sr_xCuO_4$ (Figs. 5 and 6).

Thus, the correlation shown in Fig. 6 may be explained, similarly to the case of NO decomposition. Since no significant chemical shifts attributable to the presence of Cu^{3+} were observed by XPS for $La_{2-x}Sr_xCuO_4$,[14] the oxidation number of copper on the surface is two even when it is greater than two in the solid bulk. When N_2O is adsorbed at oxygen vacancies or coordinatively unsaturated Cu^{2+} ions, a partial electron transfer occurs.[5,11]

$$Cu^{2+} + N_2O \rightarrow Cu^{(2+\delta)+} - N_2O^{\delta-}.$$

Then, the N–O bond of N_2O tends to dissociate easily. As catalyst which has the greater AON of copper tends to facilitate the electron transfer, the activity increases with the AON of Cu. A somehow similar explanation has been given for the decomposition of N_2O on $La_{1.85}Sr_{0.15}CuO_4$, La_2CuO_4, and $CuAlO_2$;[19] the presence of Cu^{2+}/Cu^{3+} and oxygen vacancy in $La_{1.85}Sr_{0.15}CuO_4$ is the main reason of its high activity.

(2) Effects of 3d Elements at B-Site. The catalytic activities of $LaMO_3$ for oxidation reactions are principally determined by the B-site elements.[11,12,16] In the cases of the oxidations of CO, CH_4, and C_3H_8, twin-peak patterns with Co and Mn at the peaks are obtained as in the case of simple oxides of M elements.[12,16] These patterns have been explained by either the electronic state of the d electron of the B-site ion, the binding energy of M–O band, or the stabilization energy of crystal field.[11—13] Although it is not certain which factor is essential, the readiness of the reduction–oxidation cycle of the B-site ion under the reaction atmosphere probably determines the catalytic activity for oxidation

reactions.

In this study of N_2O decomposition, a one-peak pattern with the peak at Co is observed (Fig. 7). One-peak pattern with a peak at Co (1073 K) or Fe (973 K) has also been reported for NO decomposition over $LaMO_3$,[18] although the differences in the activity of the catalyst were relatively small. Anyhow, it is notable that $LaMnO_3$ is active for the oxidation of CO, CH_4, and C_3H_8 but not active for N_2O or NO decomposition.

$LaMnO_3$ is known to be a metal-ion deficient mixed oxide,[21,23] the actual stoichiometry being $LaMnO_{3+\delta}$. In the case of N_2O or NO decomposition, the reaction conditions are always in oxidizing atmosphere, while reducing reagents are present in the case of catalytic oxidation reactions. Therefore, the possible reason why $LaMnO_3$ was less active for N_2O and NO decomposition is that the surface oxygen vacancy or the coordinatively unsaturated Mn ion is hardly generated on the surface of $LaMnO_3$.

On the other hand, although $LaCoO_3$ is usually stoichiometric, it has tendency to be oxygen-deficient as reported previously.[22,24] This may explain the high catalytic activity of $LaCoO_3$ for N_2O and NO decomposition.

The authors appreciate financial support in part by New Energy and Industrial Technology Development Organization (NEDO)/Research Institute of Innovative Technology for the Earth (RITE), the Grant-in-Aid for Scientific Research from the Ministry of Education, Science and Culture, and the Asahi Glass Foundation.

References

1) C. G. Tokoudis and L. D Schmidt, *J. Catal.*, **80**, 274 (1983).
2) W. M. Kalback and C. M. Shepcevich, *Ind. Eng. Chem. Fundam.*, **17**, 165 (1978).
3) E. R. S. Winter, *J. Catal.*, **15**, 144 (1969).
4) M. Kobayashi and H. Kobayashi, *Catal. Rev.*, **10**, 139 (1974).
5) A. Cimino, V. Indovina, F. Pepe, and F. S. Stone, *Gazz. Chim. Ital.*, **103**, 935 (1973).
6) C. S. Swamy and J. Christopher, *Catal. Rev.-Sci. Eng.*, **34**, 409 (1990).
7) G. I. Panov, V. I. Sobolev, and A. S. Kharitonov, *J. Mol. Catal.*, **61**, 85 (1990).
8) M. Tabata, H. Hamada, Y. Kindaichi, U. Sasaki, and T. Ito, *Chem. Express*, **7**, 77 (1992).
9) J. N. Armor, *Appl. Catal. B: Environ.*, **1**, 221 (1992).
10) Y. Li and J. N. Armor, *Appl. Catal., B: Environ.*, **1**, L21 (1992).
11) L. G. Tejuca, J. L. G. Fierro, and J. M. D. Tascon, *Adv. Catal.*, **36**, 237 (1989).
12) N. Yamazoe and Y. Teraoka, *Catal. Today*, **8**, 175 (1990).
13) M. Misono, "Future Opportunities in Catalytic and Separation Technology," ed by M. Misono, Y. Moro-oka, and S. Kimura, Elsevier, Amsterdam (1990), p. 13.
14) H. Yasuda, T. Nitadori, N. Mizuno, and M. Misono, *Bull. Chem. Soc. Jpn.*, **66**, 3492 (1993).
15) J. M. Longo and R. A. Mccauly, *J. Am. Ceram. Soc.*, **69**, 699 (1986).
16) T. Nitadori, T. Ichiki, and M. Misono, *Bull. Chem. Soc. Jpn.*, **61**, 621 (1988).
17) S. Shin, H. Arakawa, Y. Hatakeyama, K. Ogawa, and K. Shimomura, *Mater. Res. Bull.*, **14**, 633 (1979).
18) Y. Teraoka, H. Fukuda, and S. Kagawa, *Chem. Lett.*, **1990**, 1.
19) J. Christopher and C. S. Swamy, *J. Mol. Catal.*, **52**, 69 (1990).
20) M. Nakamura, S. Fujita, and N. Takezawa, *Shokubai*, **34**, 340 (1992).
21) B. C. Tofield and W. R. Scott, *J. Solid State Chem.*, **14**, 395 (1974).
22) S. C. Sorenson, J. A. Wronkiewicz, L. B. Sis, and G. P. Wirtz, *Ceram. Bull.*, **53**, 446 (1974).
23) T. Nitadory, S. Kurihara, and M. Misono, *J. Catal.*, **98**, 221 (1986).
24) T. Nakamura, M. Misono, and Y. Yoneda, *Bull. Chem. Soc. Jpn.*, **55**, 394 (1982).